Asociación Argentina
de Mecánica Computacional

Mecánica Computacional Vol XXIX, págs. 7787-7797 (artículo completo)
Eduardo Dvorkin, Marcela Goldschmit, Mario Storti (Eds.)
Buenos Aires, Argentina, 15-18 Noviembre 2010

ON THE DYNAMIC COLLAPSE OF CYLINDRICAL SHELLS UNDER HYDROSTATIC AND IMPULSIVE PRESSURE LOADINGS

Luciana Loureiro Silva and Theodoro A. Netto

Ocean Engineering Department, Federal University of Rio de Janeiro, COPPE, Rio de Janeiro, Brazil, lucianals@lts.coppe.ufrj.br, http://www.lts.coppe.ufrj.br

Keywords: Underwater Explosion, Shock Wave, Dynamic Collapse, Finite Element Model.

Abstract. The dynamic collapse of submerged cylindrical shells subjected to lateral impulsive pressure loads caused by underwater explosions is studied via coupled experimental and numerical work. The parent problem of the dynamic collapse of such structures under hydrostatic pressure is also investigated. Two sets of experiments were performed. Initially, 50.6mm outside diameter aluminum tubes with diameter-to-thickness ratio of 32.3 were tested inside a pressure vessel. Hydrostatic pressure was applied quasi-statically up to the onset of collapse in order to obtain the collapse pressure of the tubes tested. Subsequently, similar tubes were tested in a 5m x 5m x 1.6m deep water tank under various explosive charges placed at different distances. Explosive charges and standoff distances were combined so as to eventually cause collapse of the specimens. In both sets of experiments, dynamic pressure and strain measurements were recorded using a fit-for-purpose data acquisition system with sampling rates of up to 1 Mega Samples/sec per channel. In parallel, finite element models were developed using commercially available software to simulate underwater explosion, pressure wave propagation, its interaction with a cylindrical shell and the subsequent onset of dynamic collapse. The surrounding fluid was modeled as an acoustic medium, the shells as J_2 flow theory based materials with isotropic hardening, and proper fluid-structure interaction elements accounting for relatively small displacements of the boundary between fluid and structure were used. Finally, the physical explosion experiments were numerically reproduced with good correlation between results.

1 INTRODUCTION

Underwater explosion tests and analyses have been often studied to assess the vulnerability of ships and underwater structures against explosive shock loading.

The theoretical and empirical bases of underwater explosions are well established (e.g., Cole, 1948). The explosion is defined as chemical reaction in a substance which converts the original material into a gas at very high temperature and pressure. During an underwater explosion, there will be an initial shock wave propagating radially outwards to be followed by a high-pressure bubble containing hot gaseous products of the explosion. The pressure rise in the shock wave is practically instantaneous, and decreases exponentially and lasts a few milliseconds. By the time the gas bubble has expanded to its maximum radius the radiated pressure has become slightly negative. Due to water inertia the bubble overshoots its equilibrium radius, so it begins next to contract, and then undergoes a damped radial oscillation.

An exponential function is usually used to correlate the pressure and radius of the shock wave measured from the standoff point:

$$P(t) = P_0 e^{-t/\theta} \tag{1}$$

where P_0 is the peak pressure of shock wave, θ is the exponential decay constant and t is the time since the shock wave front arrived at the target point. A great amount of experimental work has been performed to find the relation between the two characteristic parameters P_0 and θ for a number of different explosive sources. Researchers have determined simple power-law relations between the peak pressure P_0, the mass W of explosive, and the radius r (distance from the standoff point). For example, for an underwater TNT explosion, the peak pressure is given by Swisdak (1978).

$$P_0 = 52.4\left(\frac{\mathrm{W}^{1/3}}{r}\right)^{1.13} \text{MPa} \tag{2}$$

and the time constant θ is

$$\theta = 0.084\mathrm{W}^{1/3}\left(\frac{\mathrm{W}^{1/3}}{r}\right)^{-0.23} \text{ms} \tag{3}$$

These relations have been validated for the domain of W and r such that P_0 lies in the range 3–140 MPa (Swisdak, 1978).

Several authors have studied the phenomena using numerical and experimental techniques. Kwon and Fox (1993) studied the nonlinear dynamic response of a cylinder subjected to a side-on, far-field underwater explosion (*undex*). Comparisons between strain gage measurements and numerical results at several different locations on the cylinder revealed a good agreement. Wardlaw and Luton (2000) examined the fluid–structure interaction mechanisms for closed-in internal and external *undex* by applying the coupled GEMINI–DYNA_N hydrocode. Hung et al. (2005a) investigated the linear and non-linear dynamic responses of cylindrical shell structures subjected to small underwater charge explosions in a water tank. Acceleration, pressure and strains at different locations were measured. Numerical analysis was also performed for the same experimental model. Liang and Tai (2006) developed a procedure to exanimate a surface ship under a shock environment. It employed the finite element method coupled with the doubly asymptotic approximation method to study the transient dynamic response of a 2000-ton patrol-boat subjected to an underwater explosion. Experimental studies with instrumented target structures, sometimes combined with high-speed imaging are essential for progress in this area, and despite the extreme

loading conditions involved, a number very informative studies have been undertaken (Brett and Yiannakopolous, 2008; Jones and Shin, 1990; Rajendra and Narasimhan, 2000; Hung et al., 2005a, Hung et al., 2005b).

These previous studies on the effect of shock loading on submerged cylinders have provided valuable information. Based on the geometry of the structure and the shock wave induced by the underwater explosion it is possible to estimate the damage imposed to the structure and, consequently, to quantify its survivability.

In this work, focus will be given to the dynamic collapse of cylindrical shells under impulse pressure loads caused by underwater explosions. The problem will be studied via coupled finite element analyses and experimental tests. Once calibrated in view of the experiments, the model is used to perform a parametric study to assess how different explosive charges and different standoff point distances combine to cause the collapse of such structures.

2 EXPERIMENTS

Nominal material and geometric parameters used in this work are as follows:

- material: aluminium;
- diameter (D): 50.6 mm;
- thickness (t): 1.57 mm;
- diameter-to-thickness ratio (D/t): 32.3;
- length (l): 655mm (for tubes tested under hydrostatic pressure) and 2000 mm for tubes tested in water tank under explosive charges.

2.1 Material Characterization

The measured engineering stress–strain curve of the tube used to manufacture all specimens is shown in Fig. 1. The curve is the average of tests on three test coupons cut in the axial direction of the tube. The average Young's modulus (E), Poisson's ratio (v), and 0.2% offset yield stresses (σ_o) are listed in Table 1.

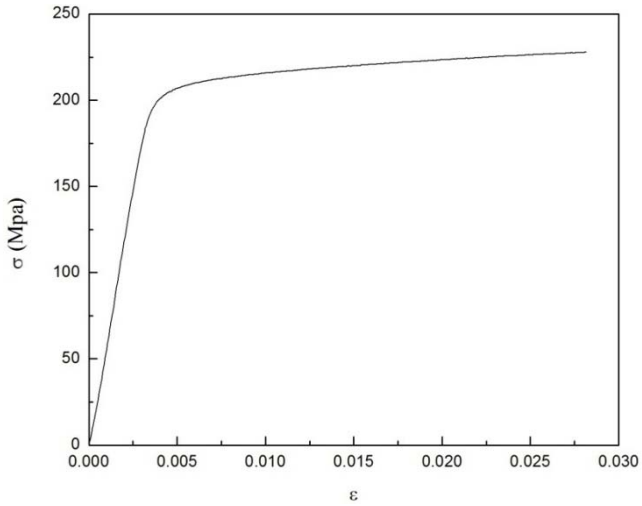

Figure 1: Engineering stress–strain curves of test specimens.

Tube	E(GPa)	ν	σ_0(MPa)
T01	56.85	0.32	208.07

Table 1: Material parameters of tube tested.

2.2 Geometric Parameters

The dimensions of each specimen were measured prior to each test. The average values for diameter (D), wall thickness (t), initial ovality and wall eccentricity are listed in Table 2. The diameter (D) was measured at twenty points equally spaced along the circumference of twenty cross-sections along the overall length. The thickness (t) at the first and last cross-sections was also measured at the same twenty angular positions, totaling forty thickness measurements. This set of data was used to calculate the ovality (Δ_0) and the wall thickness eccentricity (Ξ_0) of the measured cross-sections, defined respectively as follows (Yeh and Kyriakides, 1988) .

$$\Delta_0 = \frac{D_{max} - D_{min}}{D_{max} + D_{min}} \tag{4}$$

and,

$$\Xi_0 = \frac{t_{max} - t_{min}}{t_{max} + t_{min}} \tag{5}$$

Specimen	Tube	D(mm)	t(mm)	D/t	Δ_0(%) max.	Ξ_0(%) max.	P_{CO} (psi)
SC01	T01	50.55	1.56	32.46	0.15	1.6	549
SE01	T01	50.60	1.58	32.10	0.76	1.9	-

Table 2: Geometric parameters of pipes tested.

2.3 Collapse of pipe under hydrostatic pressure and under the effect of underwater explosion

Specimen SC01 was tested inside a pressure vessel under hydrostatic pressure in a near quasi-static volume control fashion until collapse occurred. The experimental collapse pressure was 3.79 MPa.

Subsequently, underwater explosion experiments were performed in a 5m x 5m x 1.6m water tank. Specimen SE01 was filled with air at atmospheric pressure and sealed with the use of end caps. The customized tube support apparatus built for the experimental tests is illustrated in Fig. 2. Small quantities of common explosive Pentolite/TNT (50/50) were added to a detonator to simulate the underwater explosions and shock wave propagation in the surrounding fluid.

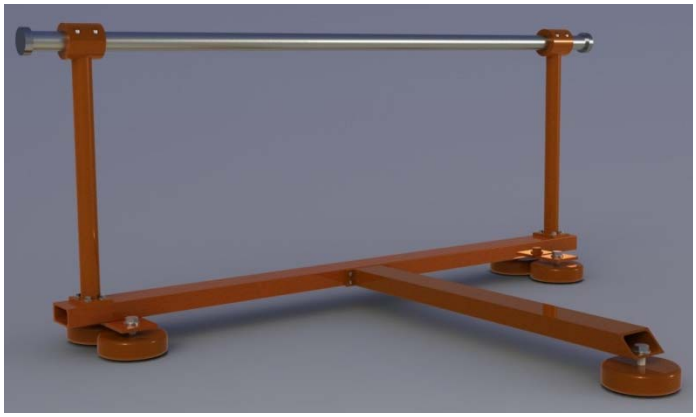

Figure 2: Support apparatus of the tube built for the experimental tests.

The dynamic pressure sensors used to measure the pressure waves were PCB tourmaline underwater blast ICP pressure sensors model W138A05 and W138A10. The nominal sensitivity of each blast sensor is approximately 1.0 mV/psi over the measurement range of 0–5000 psi and 2.0 mV/psi over the measurement range of 0–10000 psi (uncertainty of ±1.3%. Four sensors were connected to a PCB model 482A21 sensor signal conditioner. Signals were recorded using a fit-for-purpose data acquisition system with sampling rates of 1 MS/s per channel.

Fig. 3 shows a schematic view of the instrumentation layout of the cylinder and the pressure sensors in the tank. The cylinder is subjected to various explosive charges placed at different distances as shown in Table 3. Explosive charges and standoff distances were combined so as to eventually cause collapse of the specimens. For comparison, the dynamic response of the same tube under the same shock loading was numerically reproduced.

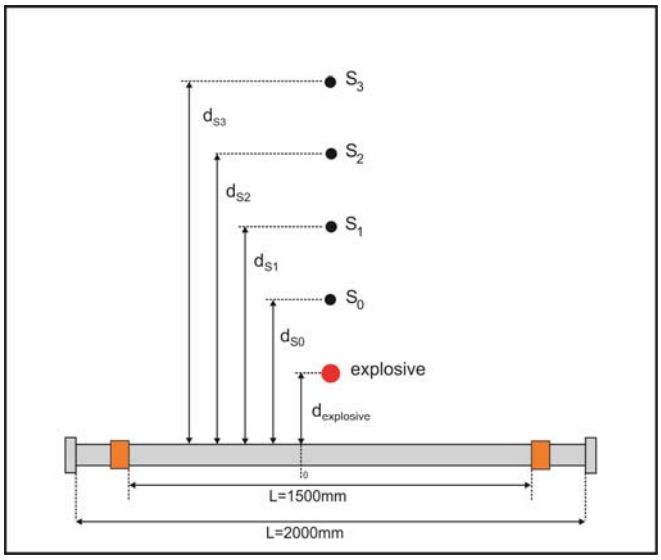

Figure 3: Schematic of instrumentation layout (top view).

Test	Specimen	Additional mass explosive* (g)	d_{charge} (m)	d_{S0} (m)	d_{S1} (m)	d_{S2} (m)	d_{S3} (m)
T01	No	0.0g	0.5750	1.150	1.725	2.300	2.875
T02	SE01	0.0g	0.5750	1.150	1.725	2.300	2.875
T03	SE01	0.5g	0.5750	1.150	1.725	2.300	2.875

T04	SE01	1.5g	0.5750	1.150	1.725	2.300	2.875
T05	SE01	2.0g	0.5750	1.150	1.725	2.300	2.875
T06	SE01	2.5g	0.5750	1.150	1.725	2.300	2.875
T07	SE01	3.0g	0.5750	1.150	1.725	2.300	2.875
T08	SE01	3.0g	0.300	-	0.600	-	-
T09	SE01	3.0g	0.250	-	0.500	-	-
T10	SE01	3.0g	0.200	-	0.400	-	-
T11	SE01	3.0g	0.150	-	0.300	-	-

Table 2: Configuration tests. (*) Additional mass to the detonator which is composed of 0.3g of of primary high explosive (1/3 lead styphnate + 2/3 of lead azide) plus 0.5g Pentolite.

Pressure waves were measured using the dynamic pressure sensors in all tests. Typical results are shown in Fig. 4 (test T01). The maximum pressure recorded with sensor S0 rises sharply to 6.90 MPa, dropping to approximately to zero pressure after about 0.5 ms. The up-and-down behavior observed as the pressure tends to zero can be attributed to the waves reflected by the tank walls and apparatus. The signals recorded at other locations have similar behavior, but with considerably lower pressure peaks. Sensor S1 gives a maximum pressure of 2.45 MPa, sensor S2 of 1.58 MPa and sensor S3 of 1.30 MPa. Similar pressure-time histories were observed for the other charge weights (not shown here).

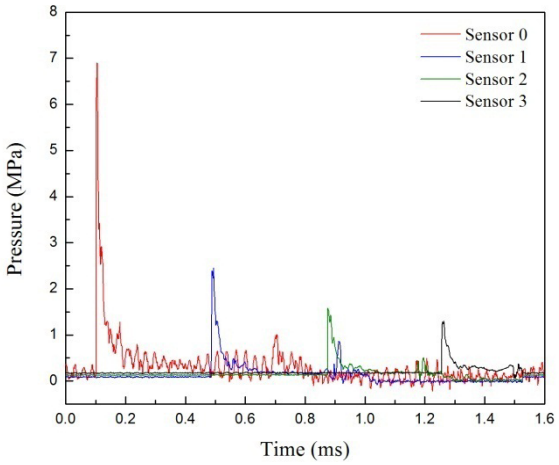

Figure 4: Complete pressure record for explosive weight (test T01).

The shock wave peak pressure values at a distance of 0.575 m from the explosive charge are presented in Fig. 5(a) for various explosive weights (tests T02 to T07 in Table 3). Fig. 5(b) shows the maximum shock wave peak pressure values on the pipe surface for various standoff distances using the same explosive weight. Usually, tube collapse occurred for a standoff distance of 0.15m and explosive weight of 3g. Two collapsed specimens tested in this scheme are shown in Fig. 6.

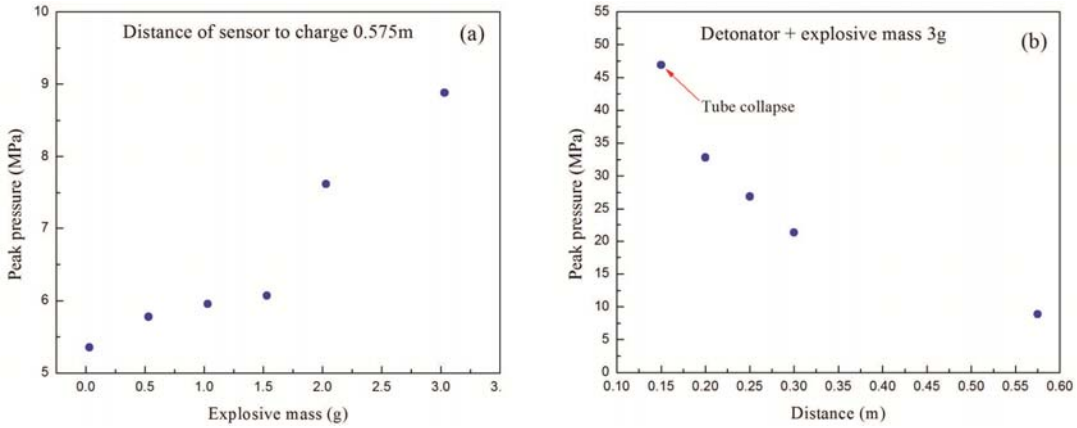

Figure 5: Peak pressure in function of (a) explosive mass and (b) standoff distance.

Figure 6: Photos of collapsed tube SE01 after being subjected to 3g explosive from distance of 0.150m (test T11): (a) front view and (b) transverse view.

3 NUMERICAL MODEL

3.1 Collapse Of Pipes Under Hydrostatic Pressure

In parallel with the experimental program, finite element models were developed within the framework of the nonlinear finite element code ABAQUS (version 6.9-1). The pipe was discretized with 3-D bricks (C3D20R) with reduced integration. The appropriate number of elements in the radial (thickness), circumferential, and longitudinal directions were established by convergence studies. Considering the symmetric condition in both longitudinal and circumferential directions, only one quarter tube was modelled. Fig. 7 shows a typical finite element mesh used in the collapse calculations. The tube is modelled as an isotropic elastic–plastic material that obeys J_2 flow theory, and incremental plasticity using actual stress–strain data is employed. Thus, true stress–strain data measured are directly provided to the FE analysis. Additionally, pipe out-of-roundness (Δ_0) is assumed uniform along the length. The maximum value measured among all cross-sections was adopted in the calculations. Pressure was applied on the tube external surface incrementally using the Riks path following method in order to obtain the loading history over the pressure maxima.

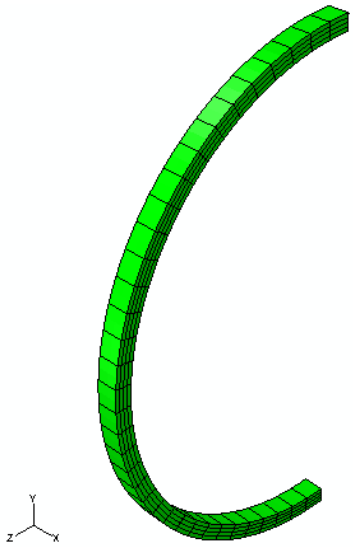

Figure 7 Finite element mesh for a quarter tube.

Calculated collapse pressure was 3.89 MPa. A very good correlation with the experimental result was obtained, with a relative error of approximately 3%.

3.2 Underwater Explosion

Numerical analysis was performed using three-dimensional finite element models that simulate underwater explosion, pressure wave propagation, its interaction with a cylindrical shell and the subsequent onset of dynamic collapse. The models were developed so as to reproduce the physical experiments.

The pipe was discretized with S4R shell elements, usually consisting of 23520 nodes and 7840 elements. The external fluid was modelled with four node reduced integration acoustic elements AC3D4R. The outer boundary of the external fluid is represented by a non-reflecting cylindrical surface of radius 0.151 m. The surrounding fluid is thus assumed as an acoustic medium in which the shockwave generated by an underwater explosion propagates and its energy leaves the mesh through a non-reflecting boundary. Multiple layers having different internal radius were used to define the external fluid, being more refined around the pipe region and presenting a coarser mesh at increasing distances from the pipe. Only small displacements of the fluid are allowed. One half of the fluid mesh is omitted from Fig. 8 for better visualization of the mesh. The experimental pressure–time history of a given shockwave can be used as tabular input for the analyses.

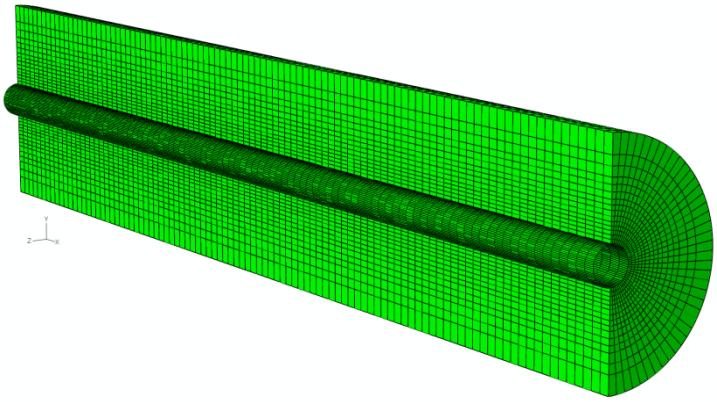

Figure 8: Finite element mesh (one half of the fluid mesh is omitted).

Interaction between shell structure and acoustic medium was modeled using an approximate technique called the doubly asymptotic approximation (DAA) - for details see Kwon and Fox (1993).

The out-of-roundness of the intact pipes was simulated through a local imperfection placed in the neighbourhood of $x = 0$. The imperfection has the form:

$$w_0(\theta) = -\Delta_0 exp\left[-\beta\left(\frac{x}{D}\right)^2\right] cos2\theta \tag{6}$$

where w_0 is the radial displacement and θ is polar angular coordinate measured from the y axis. The maximum amplitude of the imperfection is Δ_0 and β is a multiplier parameter that determines the extent of the imperfect area (typically was one to two pipe diameters).

The pressure input used in the analyses were obtained from sensor S0 used in tests T02 to T07 and sensor S1 in T08 to T11. These sensors are the same distance that the explosive is on the tube (standoff distance). For example, Fig. 9 illustrates the time history of an incident shock pressure at a standoff distance of 15cm (test T11).

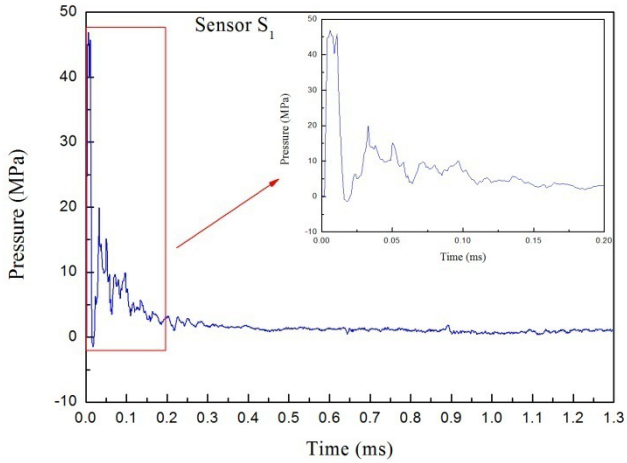

Figure 9: The time history of the measured pressure at a standoff distance of 0.150 m.

The equivalent plastic strain (PEEQ) histories at the nearest point to the charge are plotted in Fig. 10 for all analyses corresponding to each experimental test. One can notice that the equivalent plastic strain is equal to zero in all cases in which the standoff distance was 0.575 m. Small plastic deformations were observed for a standoff distance of 0.300 m. As expected, PEEQ increases with decreasing standoff distance, with very large induced plastic strains in case of pipe collapse (see test T11, standoff distance = 0.150 m – Fig. 10).

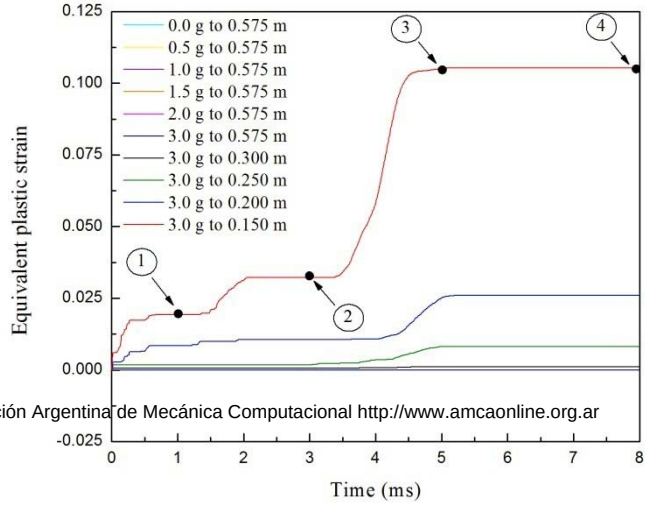

Figure 10: Comparison of equivalent plastic strain results for all configuration tests at position nearest the charge.

Fig. 11 illustrates a sequence of deformed configurations for test T11 using the incident shock pressure shown in Fig. 9 and standoff distance equal to 0.150 m (events 1 to 4 are marked in Fig. 10).

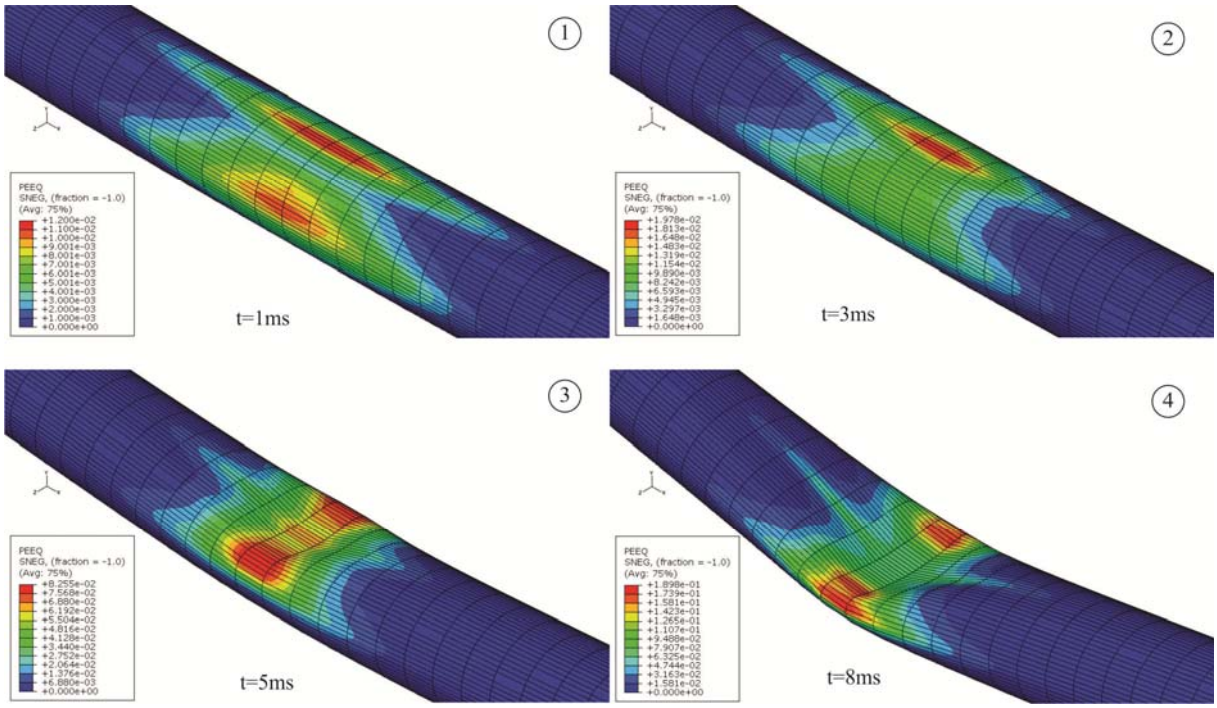

Figure 11: Sequence of equivalent plastic strain at t = 1, 3, 5 and 8 ms (standoff distance = 0.150 m and incident shock pressure show in Fig. 9).

For the sake of comparison, Fig. 12 shows the difference between the maximum equivalent plastic strain at time of 8 ms obtained from the tests T10 (standoff = 0.200 m) and T11 (standoff = 0.150 m). In the first case, the pipe does not collapse although some plastic deformation is caused by the impulsive pressure wave (Fig. 12a). Moving the charge 5 cm closer causes collapse of the specimen, as seen in Fig. 12(b). These results are corroborated by the experiments, i.e., for this particular explosive change, dynamic collapse only occurred when the standoff point was set equal to 0.15 m.

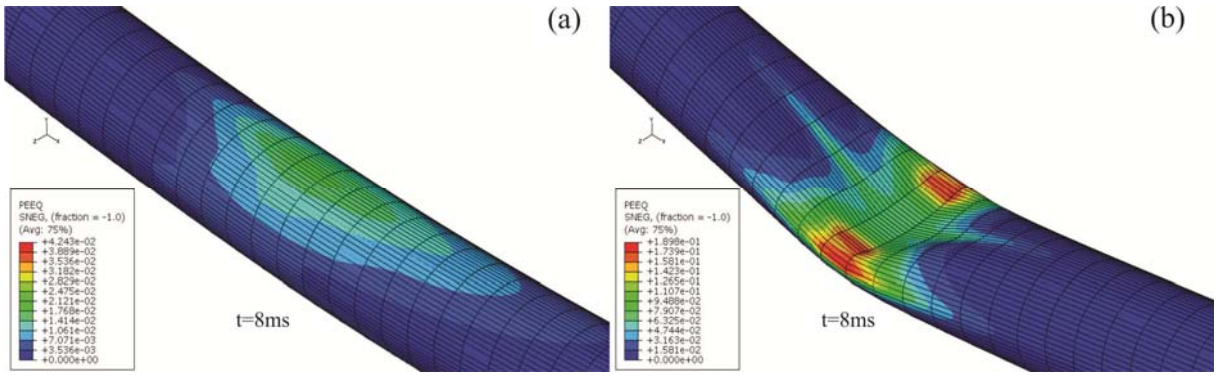

Figure 12: Comparison between the maximum equivalent plastic strain obtained from the tests T10 (standoff = 0.200 m) and T11 (standoff = 0.150 m).

4 FINAL REMARKS

Small-scale steel pipe specimens were fabricated and experimentally tested under static and dynamic (impulsive) pressure loads. Numerical models based on the finite element method, incorporating nonlinear kinematics and plasticity, were developed to simulate the physical experiments. In the case of dynamic pressure loads caused by underwater explosions, the surrounding fluid was approximated by an acoustic medium with limited control volume and non-reflecting boundaries. Fluid-structure interaction was considered through appropriate model that accounts for small displacements of the solid. Despite of this limitation, numerical and experimental results presented very good correlation. Very small displacements are indeed observed at the onset of collapse of cylindrical shells subjected to pressure loads. This validates the approximation of relative small displacements between fluid and structure used in the analyses for the calculation of the combinations between explosive charges and standoff distances that cause pipe collapse. It should be noticed that in order to reproduce the post collapse behavior and inherent large pipe displacements one should use Lagrangean-based formulations not considered in this work.

REFERENCES

Brett J.M. and Yiannakopolous G. A study of explosive effects in close proximity to a submerged cylinder. *International Journal of Impact Engineering*, 35:206–225, 2008.

Cole R.H. *Underwater explosions*. Princeton University Press, 1948.

Hung C.F., Hsu, P.Y., and Hwang-Fuu J.J. Elastic shock response of an airbacked plate to underwater explosion. *International Journal Impact Engineering*, 31:151–168, 2005a.

Hung C.F., Lin B.J., Hwang-Fuu J.J., and Hsu P.Y. Dynamic response of cylindrical shell structures subjected to underwater explosion. *Ocean Engineering*, 36:564–577, 2009b.

Jones R.A. and Shin Y.S. Experimental investigation of the response and failure mechanisms of circular metal and composite plates to underwater explosion. *In: Proceedings of 61st shock and vibration symposium*, 163–78, 1990.

Kwon Y.W. and Fox P.K. Underwater shock response of a cylinder subjected to a side-on explosion. *Computers & Structures*, 48(4):637–46, 1993.

Kyriakides S., Dyau J.Y., and Corona E. *Pipe collapse under bending, tension and external pressure (BEPTICO)*. Computer Program Manual, University of Texas at Austin, Engineering Mechanics Research Laboratory Report no. 94/4, 1994.

Liang C.C. and Tai Y.S. Shock responses of a surface ship subjected to noncontact underwater explosions. *Ocean Engineering*, 33:748–772, 2006.

Rajendran R., and Narasimhan K. Underwater shock response of circular HSLA steel plates. *Shock Vibration*, 7:251–62, 2000.

Swisdak M.M., *Explosion effects and properties: Part II - Explosion effects in water*. NSWC/WOL Tech. Report TR-76-116, 1978.

Wardlaw A.B. and Luton J.A. Fluid–structure interaction mechanisms for close-in explosions. *Shock and Vibration* 7:265–275, 2000.

Yeh M.K., and Kyriakides S. On the collapse of inelastic thick-walled tubes under external pressure. *Journal of Energy Resources Technology*, 108:35-47, 1988.